Cell

FBXL21 Regulates Oscillation of the Circadian Clock through Ubiquitination and Stabilization of Cryptochromes

Arisa Hirano,[1] Kanae Yumimoto,[2] Ryosuke Tsunematsu,[2] Masaki Matsumoto,[2] Masaaki Oyama,[3] Hiroko Kozuka-Hata,[3] Tomoki Nakagawa,[1] Darin Lanjakornsiripan,[1] Keiichi I. Nakayama,[2,*] and Yoshitaka Fukada[1,*]

[1]Department of Biophysics and Biochemistry, Graduate School of Science, The University of Tokyo, 7-3-1 Hongo, Bunkyo-ku, Tokyo 113-0033, Japan

[2]Department of Molecular and Cellular Biology, Medical Institute of Bioregulation, Kyushu University, 3-1-1 Maidashi, Higashi-ku, Fukuoka, Fukuoka 812-8582, Japan

[3]Medical Proteomics Laboratory, Institute of Medical Science,The University of Tokyo, 4-6-1 Shirokanedai, Minato-ku, Tokyo 108-8639, Japan

*Correspondence: nakayak1@bioreg.kyushu-u.ac.jp (K.I.N.), sfukada@mail.ecc.u-tokyo.ac.jp (Y.F.)

http://dx.doi.org/10.1016/j.cell.2013.01.054

SUMMARY

In the mammalian circadian clockwork, CRY1 and CRY2 repressor proteins are regulated by posttranslational modifications for temporally coordinated transcription of clock genes. Previous studies revealed that FBXL3, an F-box-type E3 ligase, ubiquitinates CRYs and mediates their degradation. Here, we found that FBXL21 also ubiquitinates CRYs but counteracts FBXL3. *Fbxl21*$^{-/-}$ mice exhibited normal periodicity of wheel-running rhythms with compromised organization of daily activities, while an extremely long-period phenotype of *Fbxl3*$^{-/-}$ mice was attenuated in *Fbxl3*/*Fbxl21* double-knockout mice. The double knockout destabilized the behavioral rhythms progressively and sometimes elicited arrhythmicity. Surprisingly, FBXL21 stabilized CRYs and antagonized the destabilizing action by FBXL3. Predominantly cytosolic distribution of FBXL21 contrasts with nuclear localization of FBXL3. These results emphasize the physiological importance of antagonizing actions between FBXL21 and FBXL3 on CRYs, and their combined actions at different subcellular locations stabilize oscillation of the circadian clock.

INTRODUCTION

Circadian rhythms with a period of approximately 24 hr are generated by an internal timekeeping mechanism referred to as the circadian clock (Takahashi, 1995, Dunlap, 1999). In mammals, the central circadian pacemaker in the hypothalamic suprachiasmatic nucleus (SCN) governs behavioral rhythms and coordinates peripheral clocks located in a variety of tissues (Schibler and Sassone-Corsi, 2002; Hastings et al., 2003). The mammalian circadian clocks are driven by a transcription-translation-based negative feedback loop. In the clockwork, CLOCK-BMAL1 heterodimers activate transcription of PERIODs (PER1-3) and CRYPTOCHROMEs (CRY1 and CRY2) through binding to E-box enhancer-elements (Gekakis et al., 1998; Bunger et al., 2000). Translated PER and CRY proteins associate with each other, translocate into the nucleus, and repress their own transcription through interaction with CLOCK-BMAL1 (Kume et al., 1999; Shearman et al., 2000). Among the clock proteins, CRY1 and CRY2 act as key players in the mammalian clockwork through their strong repressive activities on CLOCK-BMAL1-dependent transcription (Kume et al., 1999; van der Horst et al., 1999).

In addition to the transcriptional regulation, posttranslational modifications of clock proteins have critical roles for the circadian oscillation of the molecular clock (Toh et al., 2001; Gallego and Virshup, 2007; Nolan and Parsons, 2009; Reischl and Kramer, 2011). We previously reported a posttranslational mechanism regulating the stability of CRY2 protein. CRY2 is phosphorylated at Ser557 in a circadian manner in the mouse SCN and liver (Harada et al., 2005; Kurabayashi et al., 2006). The priming phosphorylation of CRY2 at Ser557 by DYRK1A allows subsequent phosphorylation at Ser553 by GSK-3β, and the two-step phosphorylation at the two neighboring Ser residues of CRY2 leads to its proteasomal degradation (Kurabayashi et al., 2010). On the other hand, CRY1 and CRY2 are ubiquitinated by the Skp1-Cul1-FBXL3 (SCF^{FBXL3}) ubiquitin ligase complex (Busino et al., 2007), and the interaction of CRYs with FBXL3, an F-box protein, is promoted by AMP-activated protein kinase (AMPK)-mediated phosphorylation of CRYs (Lamia et al., 2009). FBXL3-mediated ubiquitination of CRYs leads to their proteasomal degradation, and two point mutations in mouse *Fbxl3*, i.e., *After-hour* (*Afh*) and *Overtime* (*Ovtm*), each cause remarkable lengthening of the free-running period of the mouse behavioral rhythms (Siepka et al., 2007; Godinho et al., 2007). However, CRY2-FBXL3 interaction and FBXL3-mediated CRY2 degradation do not require Ser557/Ser553 phosphorylation of CRY2 (Kurabayashi et al., 2010). Thus, CRY proteins are subject

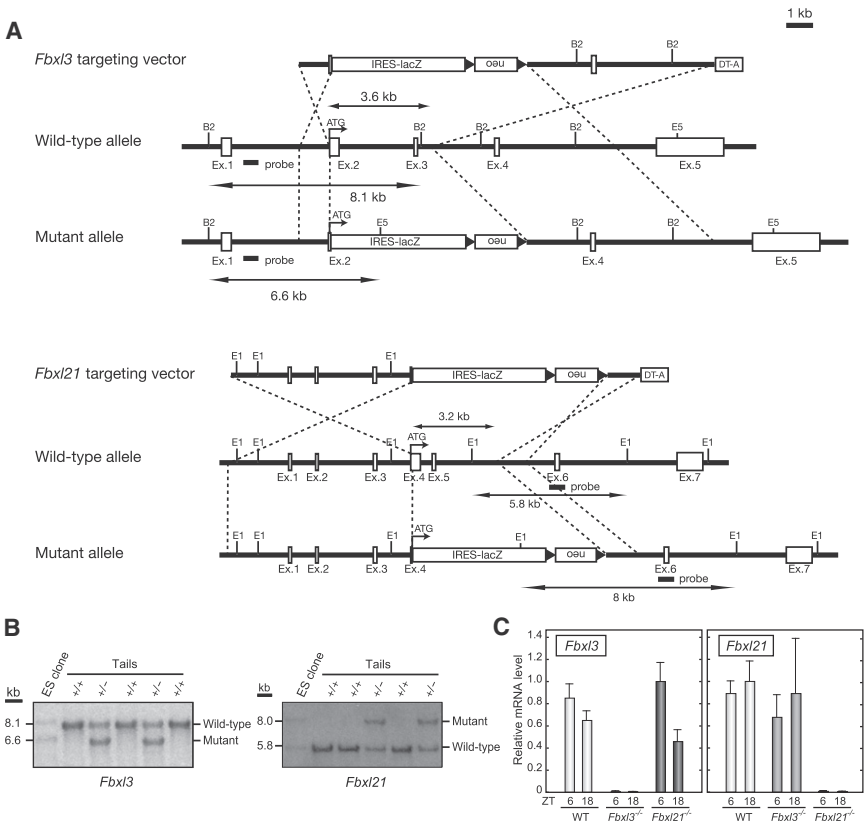

Figure 1. Generation of *Fbxl3* and *Fbxl21* Knockout Mice

(A) Targeting vectors for generation of *Fbxl3* knockout mice (*Fbxl3*$^{-/-}$) and *Fbxl21* knockout mice (*Fbxl21*$^{-/-}$).

(B) Southern blotting analysis of genomic DNA from tails of mice with the indicated genotypes for *Fbxl3* (left) or *Fbxl21* (right). The DNA was digested with BglII and EcoRV for *Fbxl3* or with EcoRI for *Fbxl21* genotyping. Hybridized probes are indicated in (A).

(C) *Fbxl3* (left) or *Fbxl21* (right) mRNA levels in the mouse liver quantified by real-time PCR. Data are means + SEM (n = 3) for wild-type and *Fbxl21*$^{-/-}$ mice and means + SD (n = 2) for *Fbxl3*$^{-/-}$ mice.

to degradation through at least two distinct pathways, postulating the involvement of another E3 ligase in the phosphorylation-dependent degradation of CRY2. Hence, we focused our attention on FBXL21, which is most similar in sequence to FBXL3 (84% amino acid sequence identity) among the F-box-type E3 ubiquitin ligase family (Jin et al., 2004; Dardente et al., 2008). Despite the similarity between these FBXL proteins, the physiological role of FBXL21 in the circadian clockwork remains to be elucidated (Dardente et al., 2008).

In this study, we show that FBXL21 ubiquitinates CRYs and that, surprisingly, FBXL21 stabilizes CRYs. FBXL21 localizes predominantly in the cytosol, whereas FBXL3 is present in the nucleus. Hence, the function and cellular distribution of FBXL21 form a sharp contrast with those of FBXL3 responsible for CRY protein degradation. The double knockout of *Fbxl3* and *Fbxl21* alleviated the circadian period-lengthening phenotype of *Fbxl3* knockout mice, further supporting their antagonizing actions on CRYs. Importantly, the double knockout destabilized the central clock in the SCN and progressively perturbed rhythmicity of the circadian behaviors in constant darkness. The antagonizing actions of *Fbxl3* and *Fbxl21* on CRY proteins have a critical role for robust oscillation of the mammalian circadian clock.

RESULTS

Generation of *Fbxl3* and *Fbxl21* Knockout Mice

Afh and *Ovtm* are two point-mutant alleles of *Fbxl3* (Siepka et al., 2007; Godinho et al., 2007). To evaluate the in vivo roles of *Fbxl3* and its closely related paralog, *Fbxl21*, we generated knockout mice lacking *Fbxl3* and/or *Fbxl21*. We created targeting vectors, in which IRES-*lacZ* and *neo* cassettes were introduced into the coding region of *Fbxl3* or *Fbxl21* gene (Figure 1A). Germline transmission of the mutant allele was confirmed by Southern blot analysis (Figure 1B). Heterozygous offspring crossed with C57BL/6 mice for at least seven generations were intercrossed to produce *Fbxl3* or *Fbxl21* knockout mice. In both cases, the genotypic distribution of the offspring followed Mendelian inheritance, and all the knockout mice used in the present study were normal in appearance. The messenger RNA (mRNA) levels of *Fbxl3* and *Fbxl21* in the liver of wild-type, *Fbxl3*$^{-/-}$, and *Fbxl21*$^{-/-}$ mice were analyzed by real-time PCR. *Fbxl3* or *Fbxl21* deficiency had no significant effect on the expression levels of *Fbxl21* or *Fbxl3*, respectively, when compared to their mRNA levels in the wild-type liver (Figure 1C).

Fbxl3 and *Fbxl21* Are Essential for Normal Behavioral Rhythms

We examined the effects of deficiencies of *Fbxl3* and/or *Fbxl21* on the behavioral rhythms of mice by monitoring their wheel-running activities (Figures 2A–2D). *Fbxl3* null mice apparently entrained to the 12L:12D (LD) cycle, although the onset of active phase was abnormally delayed from the light-to-dark transition (Figure 2E; Table S1 available online). In constant darkness (DD), *Fbxl3*-deficient mice showed rhythmic activities with a free-running period (τ_{DD}) of 27.74 ± 0.20 hr (Figure 1F and Table S1), which was significantly longer than that of their wild-type littermates (τ_{DD}: 23.77 ± 0.06 hr). Such an extremely long period in *Fbxl3*-deficient mice probably caused the delay of activity onset in LD. When transferred from DD to LD, 5 out of 14 *Fbxl3* knockout mice failed to entrain to the 24 hr cycle (Table S1) and apparently free ran as they did in DD (Figure 2C), a phenotype also observed in *Afh* mutant mice (Godinho et al., 2007). The circadian phenotype of *Fbxl3*-deficient mice (τ_{DD}: 27.74 ± 0.20 hr) was more severe than those of *Fbxl3*$^{Afh/Afh}$ (τ_{DD}: 26.5 hr, Godinho et al., 2007) and *Fbxl3*$^{Ovtm/Ovtm}$ (τ_{DD}: 26.21 hr,

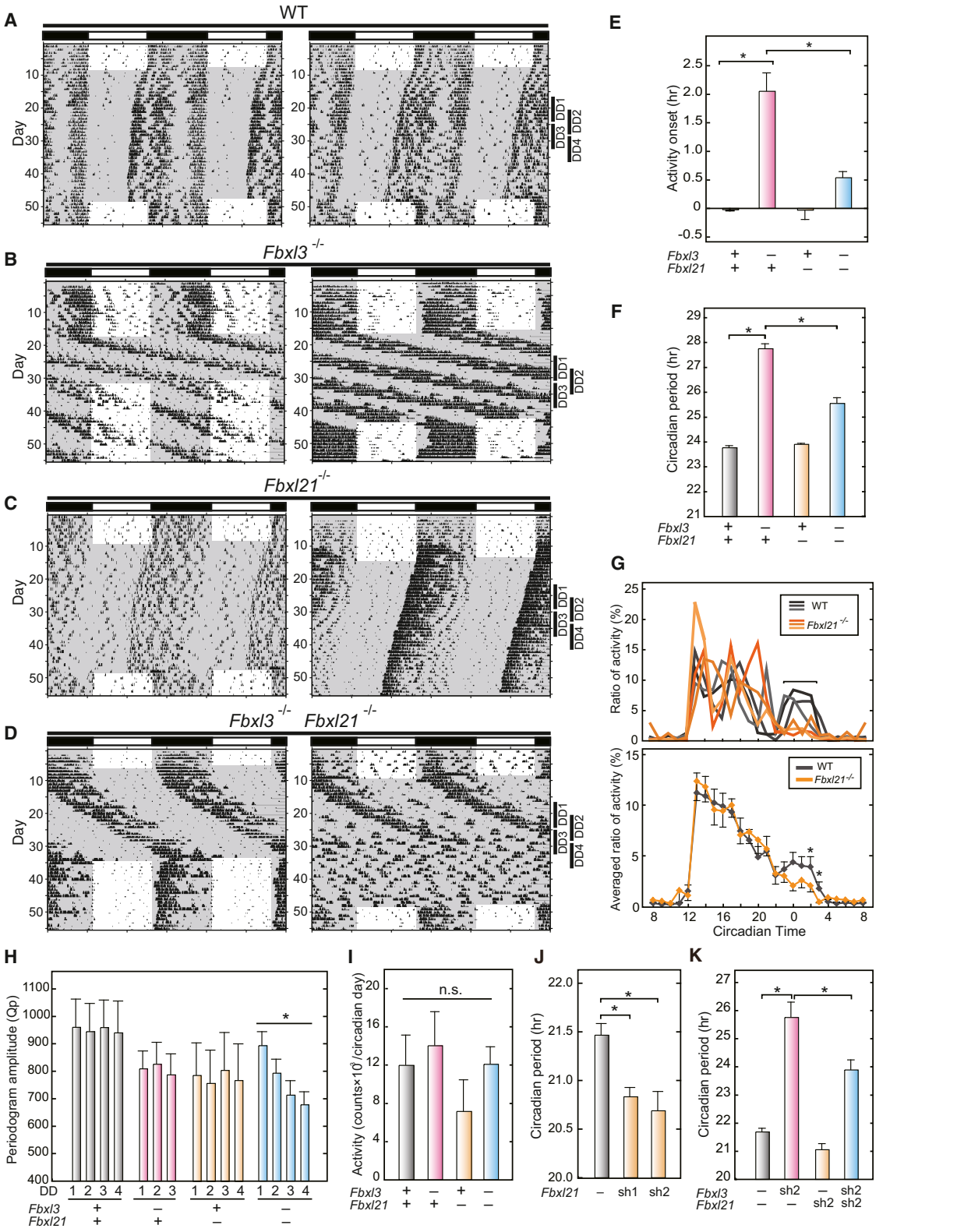

Figure 2. Wheel-Running Activity of *Fbxl3* and *Fbxl21* Knockout Mice

(A–D) Representative actograms of the wheel-running activities of wild-type (A), *Fbxl3*$^{-/-}$ *Fbxl21*$^{+/+}$ (B), *Fbxl3*$^{+/+}$ *Fbxl21*$^{-/-}$ (C), and *Fbxl3*$^{-/-}$ *Fbxl21*$^{-/-}$ (D). Mice were entrained to LD cycle for at least 5 weeks, transferred to DD, and then transferred to LD again.

(legend continued on next page)

Siepka et al., 2007). Thus, *Fbxl3* plays an important role in the regulation of the oscillation speed of the circadian clock in mice.

On the other hand, *Fbxl21*-deficient mice exhibited no significant difference from their wild-type littermates in both the free-running period in DD (Figure 2F) and activity onset in LD (Figure 2E). However, an alteration in the daily activities was obviously observed in *Fbxl21* null mice: During the active period, wild-type mice showed two peaks of activity bouts at early and late night, the latter of which was eliminated in *Fbxl21*-deficient mice (Figure 2G). This observation implies an involvement of *Fbxl21* in the SCN clock regulating temporal organization of the daily activities.

The strong phenotype of *Fbxl3* null mice in behavioral rhythm (τ_{DD}: 27.74 ± 0.20 hr) was significantly attenuated in *Fbxl3*/*Fbxl21* double-knockout mice (Figures 2D and 2F; τ_{DD}: 25.59 ± 0.15 hr). The abnormal delay of the activity onset observed in *Fbxl3* knockout mice in LD was also alleviated in the double-knockout mice (Figure 2E). However, we found that the double-knockout mice exhibited unstable behavioral rhythms in DD, although all of *Fbxl3* single-knockout mice showed rhythmic behaviors in DD: three out of ten *Fbxl3*/*Fbxl21* knockout mice were initially rhythmic but became arrhythmic within a few weeks after they were transferred to DD (Figure 2D, right panel; Table S1). We estimated the robustness of the behavioral rhythms for all the mice by the chi square periodogram procedure, where robustness is expressed as the Qp statistic reflecting the strength or regularity of a rhythm (Sokolove and Bushell, 1978). The double-knockout mice showed a progressive decline in Qp statistic during days 9–28 in DD (Figure 2H). This vulnerability was not observed in *Fbxl3* and *Fbxl21* single-knockout mice (Figure 2H; Table S1). It is therefore evident that *Fbxl3*/*Fbxl21* double deficiency destabilized the circadian oscillator in the SCN with no significant effect on the daily levels of wheel-running activity (Figure 2I). We conclude that the combined actions of *Fbxl21* and *Fbxl3* play a key role in the maintenance of both the speed and the robustness of the circadian clock oscillation.

Fbxl21 Regulates the Oscillation Speed of Cellular Clocks

A role of *Fbxl21* in the cellular clock was investigated in NIH 3T3 cells. To monitor the cellular rhythms, we introduced a luciferase reporter under the regulation of *Bmal1* promoter into the cultured cells by transient transfection. Silencing of *Fbxl21* was performed by cotransfection of an expression plasmid of small hairpin RNA (shRNA) sh21-1 or sh21-2 while *Fbxl3* was knocked down with sh3-1 or sh3-2 as described by Busino et al. (2007). Among them, sh3-2 and sh21-2 abrogated the expression of FBXL3 and FBXL21, respectively, and showed no significant crossover effects with each other (Figure S1A). We found that silencing of the *Fbxl21* gene significantly shortened the period of the cellular rhythm (Figures 2J and S1B). This period-shortening phenotype was not observed in the behavioral rhythms of *Fbxl21*-deficient mice (Figure 2F). Generally, the behavioral rhythms are only marginally affected by molecular defects in clock components due to the strong coupling among the SCN neurons, whereas the phenotypes often become manifest in the circadian rhythms of dispersed cells in culture (Liu et al., 2007). It is likely that the effect of *Fbxl21* deficiency, i.e., speeding up of the molecular oscillation, is masked by the tight neuronal coupling in the SCN. On the other hand, *Fbxl3* knockdown remarkably lengthened the periods, which were conversely shortened by additional knockdown of *Fbxl21* (Figures 2K and S1B). These results are consistent with the behavioral phenotypes of the knockout mice.

Altered Molecular Rhythms in *Fbxl21* Knockout Mice

To investigate how *Fbxl21* deficiency affects the circadian clockwork, we synchronized the cellular clocks in mouse embryonic fibroblasts (MEFs) by a pulse treatment with dexamethasone (Dex). We found that CRY1 and CRY2 protein levels in *Fbxl21*-deficient MEFs were decreased and showed circadian oscillation with reduced amplitudes as compared with those in wild-type MEFs (Figures 3A and 3B). On the other hand, the peak mRNA levels of *Cry1*, *Cry2*, and *Per1* were increased in *Fbxl21* null MEFs (Figure 3C). These results suggest destabilization of CRY proteins in *Fbxl21*-deficient MEFs. In contrast, the mRNA levels of *Dbp* were decreased and *Bmal1* mRNA levels were elevated throughout the day (Figure 3C). Although *Fbxl21*-deficient mice showed rhythmic behaviors with a period indistinguishable from that of wild-type mice (Figure 2C), transcriptional control of the clock genes is remarkably perturbed in the absence of *Fbxl21*. These molecular phenotypes can be at least in part attributable to the dysregulation of CRY1 and CRY2 in *Fbxl21*-deficient cells.

(E) Activity onset in LD cycle. The time of activity onset during the 5 days in LD just before the transition to DD was determined by ClockLab software. The means of the onset times relative to the LD transition time were plotted. Error bars show SEM. *$p < 0.05$ by Tukey's test.

(F) Circadian periods of free-running activities in DD determined by chi-square periodogram. Data from days 8 through 21 in DD were used for the calculation of the circadian periods. Error bars show SEM. *$p < 0.05$ by Tukey's test.

(G) Activity profiles of *Fbxl21*$^{-/-}$ mice across the day. (Upper panel) Typical activity profiles of wild-type and *Fbxl21*$^{-/-}$ mice in DD. (Lower panel) The ratios of the hourly activities relative to the daily total activity in DD of every mouse for each genotype were shown with error bars of SEM. *$p < 0.05$ by Tukey's test. The activity onset time was defined as circadian time 12.

(H) Temporal changes in periodogram amplitude (Qp) of the wheel-running activity rhythms of the knockout mice in DD. The Qp values were determined from the activity data during the four overlapping periods of 8 days in DD (DD1: days 9–16, DD2: days 13–20, DD3: days 17–24 and DD4: days 21–28) by chi-square periodogram by using ClockLab software (Actimetrics). Error bars show SEM. *$p < 0.05$ by one-way ANOVA.

(I) The total numbers of the wheel revolutions per circadian cycle were counted during 2 weeks (days 8–21) in DD. Error bars show SEM, and n.s. indicates not significant ($p > 0.05$ by one-way ANOVA).

(J and K) Circadian periods of cellular rhythms in culture. NIH 3T3 cells were cotransfected with a luciferase reporter (*Bmal1*us0.3-luc; Kon et al., 2008) and shRNA vectors targeting *Fbxl*s (J, *Fbxl21*; K, *Fbxl3* and/or *Fbxl21*). Forty-eight hours after the transfection, the cells were treated with 0.1 μM dexamethasone for 2 hr to synchronize the cellular rhythms. The culture medium was then changed to the recording medium for recording bioluminescence signals. Circadian periods were calculated by using the data from the 2nd to the 4th peak. Error bars show SEM (n = 4, *$p < 0.05$ by Tukey's test). See also Figure S1 and Table S1.

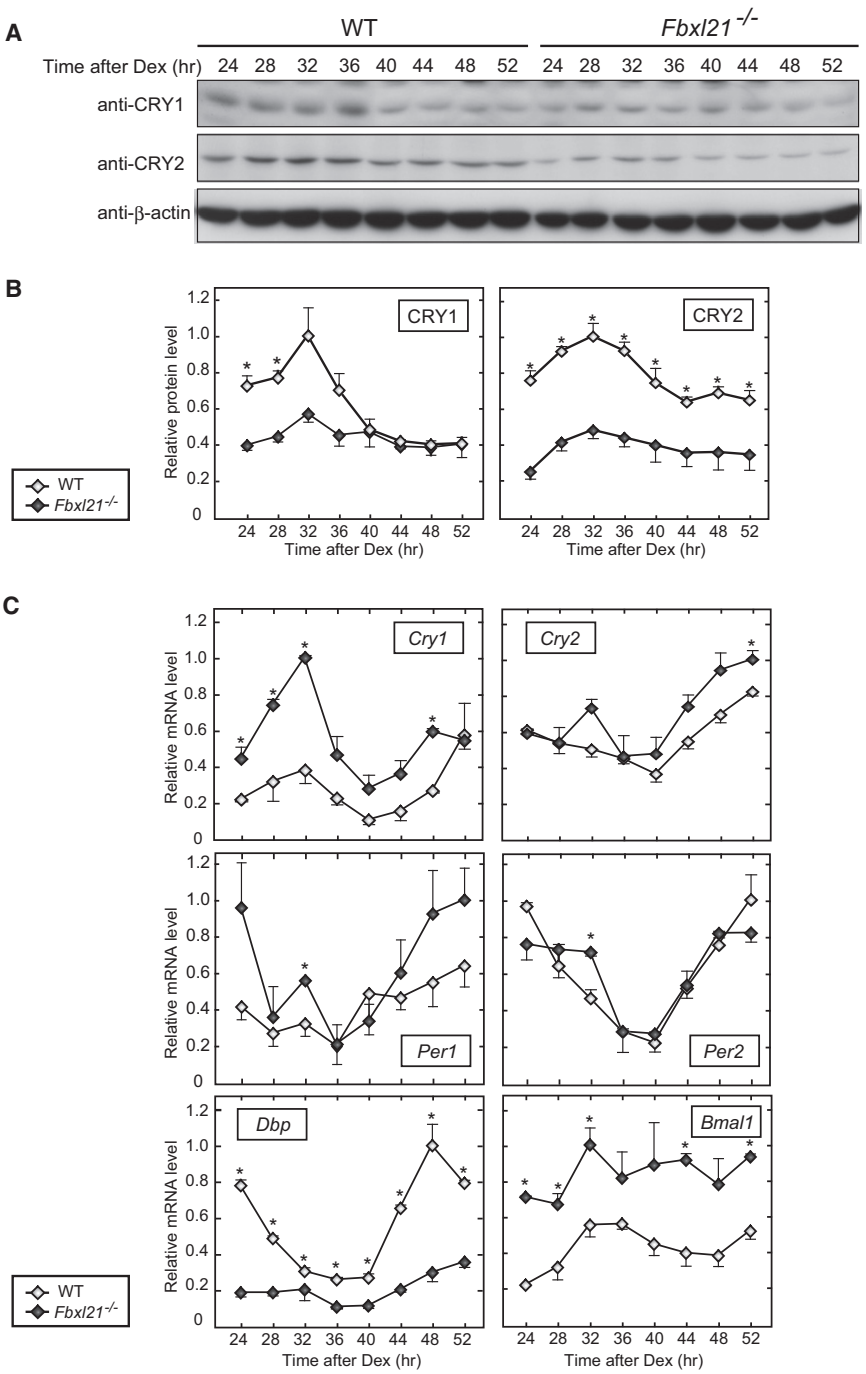

Figure 3. Circadian Expression of CRY Proteins and Clock Genes in *Fbxl21* Knockout Mice

(A) Temporal changes in CRY1 and CRY2 protein levels in *Fbxl21*$^{-/-}$ MEFs. Cellular rhythms of MEFs were synchronized by 2 hr pulse treatment of 0.1 μM dexamethasone. The cells were harvested at 4 hr intervals followed by immunoblotting with CRY1 or CRY2 antibody.

(B) The band densities of CRY1 or CRY2 in (A) within a single blot were shown as values relative to their average intensity in the blot, and the highest value was set at 1.0. Data taken from three independent experiments (i.e. three blots) were averaged and shown with error bars of SEM (n = 3, *p < 0.05 by Student's t test).

(C) Temporal changes in mRNA levels of clock genes in *Fbxl21*$^{-/-}$ MEFs. Cellular rhythms of MEFs were synchronized and total RNA was prepared at 4 hr intervals. The mRNA levels of *Cry1*, *Cry2*, *Per1*, *Per2*, *Dbp*, and *Bmal1* were quantified by real-time PCR, and the highest value among the samples was set at 1.0. Data are means with SEM (n = 3, *p < 0.05 by Student's t test).

FBXL21 Interacts with CRY Proteins

The abnormalities in temporal changes of CRY1 and CRY2 protein levels in *Fbxl21*-deficient MEFs suggest that FBXL21 shares with FBXL3 a regulatory mechanism determining CRY protein levels. We first examined the interaction of FBXL21 with CRY1 and CRY2 in cultured cells. HEK293T17 cells were transfected with expression constructs of myc-CRYs and Flag-FBXLs. We found that, just like Flag-FBXL3, Flag-FBXL21 was coimmunoprecipitated with myc-CRY1 and myc-CRY2 (Figure 4A). The interaction between myc-CRY1 and Flag-FBXL21 was verified by coimmunoprecipitation of myc-CRY1 with Flag-FBXL21 (Figure 4B).

FBXL21 Forms an SCF Complex

Members of the F-box-type E3 ubiquitin ligase family have a conserved F-box domain and a substrate recognition domain that is divergent among the members. The F-box domain is important for the formation of a Skp1-Cul1-F-box protein (SCF) complex to exert E3 ligase activity (Cardozo and Pagano, 2004). To investigate E3 ligase activity of FBXL21, we asked whether FBXL21 forms an SCF complex. Recently, the authors K.Y. and K.I.N. found that FBXL3 forms an SCF complex in a manner dependent on CRY protein (unpublished data). Based on this observation, we coexpressed myc-CRY1 or myc-CRY2 with Flag-FBXL21 or Flag-FBXL3 in HEK293T17 cells. Each myc-CRY facilitated the interaction of Skp1 and Cul1 not only with Flag-FBXL3 but also with Flag-FBXL21 (Figure 4C). It is most likely that FBXL3 and FBXL21 share the same domain for CRY binding and that the E3 ligase activities of these F-box proteins are regulated in a circadian manner through the dynamic change in CRY protein levels. Here, we noticed that Cul1 band in the precipitate with FBXLs was upshifted from the Cul1 band in the input (Figure 4C). Because NEDD8 modification of Cul1 is known to activate the SCF complex by recruiting an E2 enzyme (Pan et al., 2004), the upshifted Cul1 band might

represent its neddylated state in the SCF complex containing CRYs.

FBXL21 Ubiquitinates CRY Proteins

By using in vitro ubiquitination assay, we examined FBXL21-catalyzed ubiquitination of CRY1 in the presence of 1 of 17 E2 enzymes. We found that UBE2A or UBE2D (D1-D3: UbcH5a-5c) cooperated with not only FBXL3 but also FBXL21 in ubiquitinating CRY1 (Figures 4D and S2A). We also found an in vivo ubiquitination assay that cotransfection of Flag-FBXL3 or Flag-FBXL21 enhanced myc-CRY1 ubiquitination in HEK293T17 cells (Figures 4E and S2B) and NIH 3T3 cells (Figure S2C). Among various linkage types of ubiquitin chains, K48-linked polyubiquitination is primarily known as the protein degradation signal (Behrends and Harper, 2011). The linkage modes of FBXL21- and FBXL3-mediated ubiquitination were examined by using a mutant ubiquitin, HA-K48-Ub, in which all Lys residues except for K48 were mutated to Arg. Coexpression of Flag-FBXL3 or Flag-FBXL21 with HA-wt-Ub promoted myc-CRY1 ubiquitination to be nearly comparable to each other. On the other hand, coexpression with HA-K48-Ub attenuated myc-CRY1 ubiquitination catalyzed by FBXL21 when compared to that achieved with FBXL3 (Figure 4F). These results suggest that FBXL3 and FBXL21 elongate different types of ubiquitin chains, at least in terms of their dependence on K48 linkage. Further studies using a series of other mutant ubiquitins (such as K11-Ub, K48R-Ub, and K63-Ub) would help to identify the linkage mode of ubiquitin chains formed by FBXL21. We then asked whether CRYs are endogenous substrates of FBXL21 in NIH 3T3 cells by knockdown of *Fbxl21*. Silencing of *Fbxl21* or *Fbxl3* reduced the ubiquitinated levels of myc-CRY1 in NIH 3T3 cells (Figures 4G and S2D). These results indicate that CRY1 is an endogenous substrate for FBXL21- and FBXL3-catalyzed ubiquitination.

FBXL21 Stabilizes CRY Proteins

Ubiquitination of proteins confers various regulations on modified proteins, such as protein stability, signal transduction, enzymatic activity, and subcellular localization (Chen and Sun, 2009), whereas F-box protein-mediated ubiquitination predominantly leads the substrates to proteasomal degradation (Cardozo and Pagano, 2004). We asked whether FBXL21 regulates stabilities of CRYs by quantifying the steady-state protein levels of Flag-His-myc-tagged CRY1 (FHM-CRY1) when FBXL21 and/or FBXL3 are either overexpressed or knocked down. Overexpression of Flag-FBXL3 in HEK293T17 cells decreased FHM-CRY1 protein levels, indicating that FBXL3 promotes CRY1 degradation (Figure 5A). In contrast, overexpression of Flag-FBXL21 remarkably elevated FHM-CRY1 levels (Figure 5A). Coexpression of Flag-FBXL3 and Flag-FBXL21 restored FHM-CRY1 levels (Figure 5A), and the restoration was dose dependent for Flag-FBXL21 (Figure 5B). Similar results were obtained in experiments performed with FHM-CRY1 in NIH 3T3 cells (Figure S3A) or with FHM-CRY2 in NIH 3T3 cells (Figure S3B), suggesting that FBXL3 and FBXL21 act on CRY proteins in a mutually antagonizing manner. Myc-PER2 also binds to Flag-FBXL3 and Flag-FBXL21, possibly via indirect interaction through CRYs (Figure S3C), but myc-PER2 protein levels were mostly unaffected by coexpression with Flag-FBXL21 and/or Flag-FBXL3 (Figure S3D). An increase in Flag-FBXL21 levels had no discernible effect on Flag-FBXL3 level (Figures 5A and 5B), eliminating the possibility that the effect of overexpressed Flag-FBXL21 on FHM-CRY1 was due to the change of FBXL3 levels. Meanwhile, knockdown of *Fbxl21* by sh21-2 in NIH 3T3 cells resulted in a decrease in the steady-state levels of FHM-CRY1, whereas knockdown of *Fbxl3* increased FHM-CRY1 levels (Figure 5C). Collectively, these results indicate that CRY1 levels are regulated by FBXL21 and FBXL3 antagonistically, where FBXL21 increases CRY1 levels probably through its stabilization.

To confirm that the stability of CRY proteins is increased by FBXL21, we investigated the degradation rate of myc-CRY1 protein in cultured cells. HEK293T17 cells expressing myc-CRY1 and Flag-FBXLs were treated with cycloheximide (CHX) for 3–6 hr. Expression of Flag-FBXL3 increased myc-CRY1 degradation rate, while Flag-FBXL21 expression significantly suppressed the degradation (Figure 5D). Coexpression of Flag-FBXL3 and FBXL21 attenuated FBXL3-dependent myc-CRY1 degradation. A similar set of experiments in NIH 3T3 cells confirmed the stabilizing effect of Flag-FBXL21 on FHM-CRY1 (Figures S3E and S3F). The half-life of luciferase activity of CRY1-LUC fusion protein was markedly increased (~two-fold) by Flag-FBXL21 expression (Figure 5E), whereas the lifetime of LUC itself was unaffected by Flag-FBXL3 or Flag-FBXL21 (Figure S3G). In *Fbxl21* knockout MEFs, by contrast, the decay of CRY2 was significantly faster than that in wild-type MEFs (Figure 5F). These results demonstrate an important role of FBXL21 in CRY protein stabilization, which antagonizes the destabilizing action by FBXL3.

Ubiquitination Sites in CRY1 and CRY2

We investigated ubiquitination sites in CRY proteins by shotgun proteomic analysis of FHM-tagged CRY1 or CRY2, each of which was immunopurified from the lysates of NIH 3T3 cells (Table 1). We found a series of ubiquitinated residues in FHM-CRYs: K159, K329, and K485 in FHM-CRY1 and K125, K241, K347, K474, and K503 in FHM-CRY2 (Figure 6A, K is labeled with an asterisk). In addition, we found ubiquitinated residues in ubiquitin copurifed with FHM-CRYs: K11, K48, and K63 (Table 1). A recent study of human ubiquitin-modified proteome identified ubiquitinated residues K329 and K442 in CRY1 and K241 and K474 in CRY2 (Kim et al., 2011). The present analysis covered three out of the four ubiquitinated sites reported for human CRYs and revealed two and three additional sites in mouse CRY1 and CRY2, respectively. CRY proteins are multiply ubiquitinated in vivo, suggesting the possibility that FBXL21 and FBXL3 each catalyzes ubiquitination at a distinct subset of Lys residues in CRYs. To examine whether ubiquitination of these sites is essential for FBXL21-mediated stabilization of CRY1, we generated four mutants of myc-CRY1 (mut1–4) by introducing a K-to-R mutation, respectively, at K107, K329, K456, and K485, Lys residues which are ubiquitinated in CRY1 and/or CRY2 and are conserved between CRY1 and CRY2 (Figure 6A). Among these mutants, mut1-CRY1 (K107R) protein levels were sensitive to FBXL3-dependent degradation and, by contrast, they were unaffected by coexpression of FBXL21 in

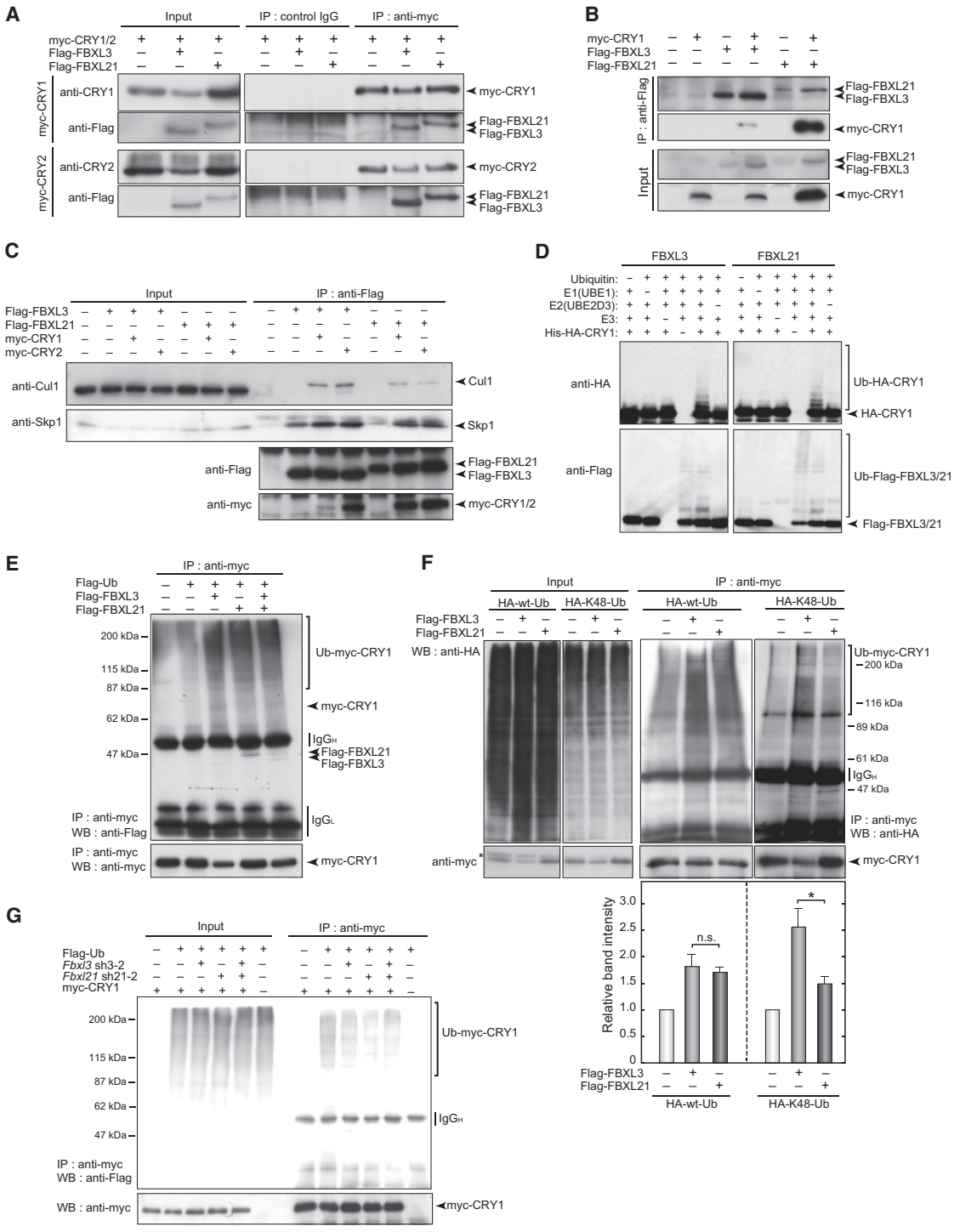

Figure 4. Interaction of FBXL21 with CRY1 and CRY2

(A) Interaction of FBXL21 with CRY1 and CRY2 in HEK293T17 cells. Cells were transfected with myc-CRYs and Flag-FBXL3 or Flag-FBXL21 expression vectors. Forty-eight hours after the transfection, the cells were harvested and lysed in IP buffer, followed by immunoprecipitation with anti-myc antibody. Immunoprecipitated product was analyzed with anti-Flag antibody.

(B) Myc-CRY1 and Flag-FBXL3 or FBXL21 were expressed in HEK293T17 cells and Flag-FBXLs were immunoprecipitated with anti-Flag antibody. Interaction of FBXL3 or FBXL21 with myc-CRY1 was detected with anti-myc antibody.

(C) FBXL21 forms SCF complex with CRY proteins. Flag-FBXLs and myc-CRY1 expression constructs were transfected into HEK293T17 cells. Interaction of FBXL21 with endogenous Cul1 and Skp1 were detected with anti-Cul1 and anti-Skp1 antibody.

(legend continued on next page)

HEK293T17 cells (Figures 6B and 6C). The other three mutant proteins (mut2–4) were mostly sensitive to both FBXL3-dependent degradation and FBXL21-dependent stabilization (Figures 6B and 6C). These observations suggest that FBXL21 stabilizes CRY1 through ubiquitination of at least one unique Lys residue K107, which is not involved in FBXL3-dependent degradation.

Subcellular Localization of FBXL21

Although the amino acid sequences of FBXL21 and FBXL3 are highly conserved, their N-terminal regions are divergent from each other. We found in this region a putative nuclear localization signal (NLS) sequence KRPR only in FBXL3 (Figure 6D). Interestingly, the NLS sequence at the corresponding position of FBXL21 is disrupted by amino acid insertion (Figure 6D). To reveal the spatial regulation of CRY ubiquitination, we examined subcellular distribution of FBXL21, FBXL3, and NLS-mut-FBXL3 that have mutations KRPR-to-AAAA at positions 22–25. Flag-FBXL3 was localized predominantly to the nucleus of HEK293T17 cells as reported by Godinho et al. (2007), whereas NLS-mutated Flag-FBXL3 was detected in the cytosol (Figures 6E and 6F), indicating that the NLS sequence is critical for nuclear localization of FBXL3. In contrast, Flag-FBXL21 was found in the cytosol with weak distribution in the nucleus (Figures 6E and 6F). Such a contrast in distribution suggests that CRY stabilities are regulated by FBXL21 and FBXL3 predominantly at different subcellular spaces. To reveal an impact of FBXL21 on nuclear and cytosolic CRYs, we investigated CRY levels in these two fractions of the mouse brain lysate prepared at ZT18 from *Fbxl3*, *Fbxl21*, and *Fbxl3*/*Fbxl21* knockout mice. As compared to wild-type, *Fbxl21*-deficient mice showed reduced levels of CRY1 and CRY2 in both the cytosol and the nucleus (Figures 6G and 6H). In *Fbxl3* null background, on the other hand, *Fbxl21* knockout decreased CRY levels only in the cytosol (Figure 6H). These findings suggest that FBXL21 protects CRYs from FBXL3-mediated degradation in the nucleus, where a minor population of FBXL21 is located. The results also imply that at least one additional CRY degradation system is operating in the cytosol, where FBXL21 plays a major role for CRYs stabilization. It is probable that the finely tuned accumulation of CRY proteins in the cytosol mediated by FBXL21 in combination with another degradation mechanism determines the proper timing of their nuclear entry (Figure 6I).

DISCUSSION

In the present study, we provide evidence for the physiological role of *Fbxl21* in the regulation of the circadian clockwork. FBXL3 and FBXL21 each bind with CRY1 and CRY2 (Figures 4A and 4B) and form an SCF complex (Figure 4C), which mediates ubiquitination of CRY proteins (Figures 4D, 4E, and 4G). Intriguingly, FBXL3 and FBXL21 regulate the stability of CRY proteins in opposite directions despite the high degree of their sequence identity (Figure 5). We found that the K-to-R mutation in CRY1 at K107, one of the ubiquitination sites identified in the present study (Table 1), attenuates FBXL21-dependent stabilization and, by contrast, has no significant effect on FBXL3-dependent degradation (Figures 6B and 6C). FBXL21 may exert its stabilizing effect on CRYs through ubiquitination of K107 in CRY1 and the corresponding residue K125 in CRY2. A CRY1 peptide, having ubiquitinated K107, was not detected in our shotgun proteomic analysis, but we speculate that substantially low ubiquitinated levels of CRY1 in NIH 3T3 cells could have hampered its detection. The Lys residues at these positions are conserved in CRY1 and CRY2 from a wide range of species, including humans, chickens, zebrafish, *Xenopus*, and Anole lizards (http://www.ensembl.org/), and CRY1 and CRY2 show the high degree of amino acid identity at the surrounding sequences, raising the possibility that K107 is a common site for ubiquitination among vertebrate CRYs in vivo.

It is well established that F-box protein-mediated ubiquitination of proteins leads to their proteasome-dependent degradation (Pan et al., 2004; Frescas and Pagano, 2008). The only reported exception to this paradigm is the stabilization of c-Myc by β-TrCP-mediated polyubiquitination, which interferes with FBXW7-mediated c-Myc ubiquitination that leads to its degradation (Popov et al., 2010). β-TrCP and FBXW7 competitively ubiquitinate the same residue on c-Myc and conjugate different linkage types of polyubiquitin chains. In this way, β-TrCP-mediated polyubiquitination protects c-Myc against FBXW7-mediated ubiquitination and degradation, and accordingly, β-TrCP is effective only in the presence of FBXW7. In the case of CRY proteins, it is likely that FBXL3 catalyzes elongation of K48-linked polyubiquitin chain, whereas FBXL21 appears to elongate a different type of ubiquitin chain (Figure 4F). In fact, we detected K11- and K63-linked structures in ubiquitins copurified with CRY proteins (Table 1). Our findings suggest FBXL21-mediated formation of a polyubiquitin chain with a K11- or K63-linked mode or a mode comprising a combination of K11, K63, or K48 linkage. CRY proteins are probably stabilized by a mechanism in which the ubiquitination of CRYs catalyzed by SCF^{FBXL21} could either compete with the formation of the K48-linked polyubiquitin chain (the degradation signal) or interfere with the function of the degradation signal.

Here, we emphasize that the phenotypes of *Fbxl21* ablation are observed even in the absence of *Fbxl3* at the behavioral level (Figure 2F) and at the molecular level (Figures 5C and 6H). These observations strongly suggest additional regulation of degradation-stabilization of CRYs operating in the cytosol, which is

(D) In vitro ubiquitination assay of CRY1. Recombinant ubiquitin, E1, E2 (UBE2D3), Rbx1, Skp1-Cul1-FBXLs (SCF^{FBXLs}), and HA-CRY1 were incubated for 2 hr at 30°C. Ubiquitinated HA-CRY1 (Ub-HA-CRY1) was detected by immunoblotting with anti-HA antibody.

(E) In vivo ubiquitination assay of CRY1. Flag-ubiquitin (Ub), myc-CRY1, and Flag-FBXLs were expressed in HEK293T17 cells. Forty-two hours after the transfection, the cells were treated with 10 μM MG132 for 6 hr. Ubiquitination of myc-CRY1 purified with anti-myc antibody was detected by anti-Flag antibody.

(F) In vivo ubiquitination assay of CRY1. HA-wt-Ub or HA-K48-Ub was coexpressed with myc-CRY1 and Flag-FBXLs in HEK293T17 cells. Forty-two hours after the transfection, the cells were treated with 10 μM MG132 for 6 hr. Ubiquitination of myc-CRY1 purified with anti-myc antibody was detected by anti-HA antibody. The intensity of the smeared bands of polyubiquitinated CRY1 was quantified. Data are means + SEM (n = 3, *p < 0.05 by Student's t test).

(G) *Fbxl21* knockdown reduced CRY1 ubiquitination. shRNA expression vectors targeting *Fbxl*s were transfected to NIH 3T3 cells and the cells were treated with 10 μM MG132 for 6 hr before harvest. Ubiquitination of myc-CRY1 purified with anti-myc antibody was detected by anti-Flag antibody. See also Figure S2.

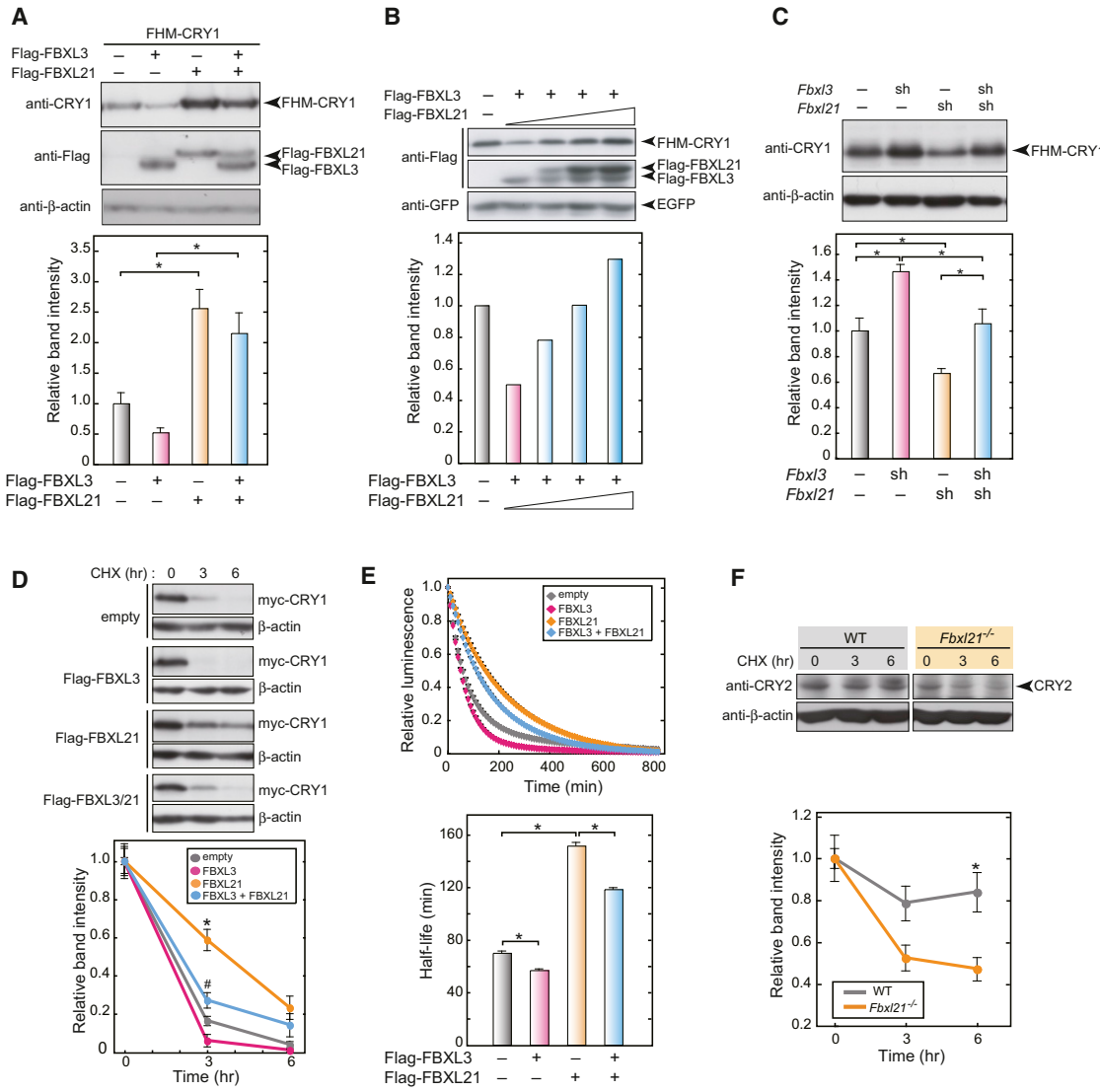

Figure 5. Effect of FBXL21 on the Stability of CRY Proteins

(A) Effect of FBXL21 on the steady-state levels of CRY1 protein. Flag-His-myc-CRY1 (FHM-CRY) and Flag-FBXL expression vectors were cotransfected to HEK293T17 cells. Forty-eight hours after the transfection, CRY1 expression levels were quantified by immunoblotting with CRY1 antibody. Data are means + SEM (n = 3, *p < 0.05 by Tukey's test).

(B) FBXL21 dose dependently restored CRY1 protein levels that were reduced by FBXL3. The amounts of the plasmid for Flag-FBXL21 expression were 0, 50, 100, and 200 ng. EGFP was used for a loading control.

(C) Effect of *Fbxl21* knockdown on the steady-state levels of CRY1 protein. shRNA expression vectors (sh3-2 or sh21-2) were transfected to NIH 3T3 cells. Seventy-two hours after the transfection, CRY1 levels were quantified by immunoblotting with CRY1 antibody. Data are means + SEM (n = 3, *p < 0.05 by Tukey's test or Dunnett's test).

(D) Degradation assay of myc-CRY1. Flag-FBXLs and myc-CRY1 were expressed in HEK293T17 cells. Forty-eight hours after the transfection, the cells were treated with 100 μg/ml CHX for 3 or 6 hr. Then, the cells were harvested, followed by immunoblotting with CRY1 antibody. CRY1 levels at time zero in each condition were normalized to 1.0. Data are means + SEM (n = 3; *p < 0.05 by Tukey's test between empty and FBXL21; #p < 0.05 by Tukey's test between FBXL3 and FBXL3+FBXL21).

(E) Degradation assay of CRY1-LUC. CRY1-LUC and Flag-FBXLs were expressed in HEK293T17 cells. Forty-eight hours after the transfection, bioluminescence levels were monitored in the recording medium containing CHX. Half-life of CRY1-LUC was calculated by fitting the data with an exponential function and shown with error bars of SEM (n = 4, *p < 0.05 by Tukey's test).

(F) Degradation assay of endogenous CRY2 in *Fbxl21*$^{-/-}$ MEFs. MEFs were treated with CHX for 3 or 6 hr and then harvested, followed by immunoblotting with CRY2 antibody. The protein levels at time zero in each genotype were normalized to 1.0. Data are means + SEM (n = 3, *p < 0.05 by Student's t test). See also Figure S3.

Table 1. Ubiquitination Sites Identified by Shotgun Proteomic Analysis

Protein[a]	Position	Ubiquitinated Peptide[b]
CRY1		
	153–177	FQTLVSK$_{159}$MEPLEMPADTITSDVIGK
	323–334	NPEALAK$_{329}$WAEGR
	484–493	MK$_{485}$QIYQQLSR
CRY2		
	114–127	LTFEYDSEPFGK$_{125}$ER
	239–245	LDK$_{241}$HLER
	341–352	NPEALAK$_{347}$WAEGK
	461–477	YIYEPWNAPESVQK$_{474}$AAK
	502–511	MK$_{503}$QIYQQLSR
Ubiquitin		
	7–27[c]	TLTGK$_{11}$TITLEVEPSDTIENVK
	43–54[d]	LIFAGK$_{48}$QLEDGR
	55–72[d]	TLSDYNIQK$_{63}$ESTLHLVLR

[a]FHM-CRY1, FHM-CRY2 or FH-LacZ purified from NIH 3T3 lysate was subjected to shotgun proteomic analysis (see Extended Experimental Procedures for details).

[b]Glycylglycine was found to be linked via an amide bond to the epsilon amino group of the lysine residue (K) underlined. These residues were assigned as the attachment sites of ubiquitin because glycylglycine is derived from its C-terminal sequence RGG after proteolysis with trypsin.

[c]A peptide detected from the analysis of CRY2.

[d]Peptides detected from the analyses of both CRY1 and CRY2.

obviously different from the dual regulation by FBXL21 and FBXL3 in the nucleus. FBXL21-mediated stabilization and the counterbalancing degradation of CRYs in the cytosol are critical for determining the accumulation rate of CRY proteins. We previously reported a CRY2 degradation mechanism dependent on Ser557/Ser553 phosphorylation in the cytosol (Kurabayashi et al., 2010). However, the binding affinity of CRY2 to FBXL21 was unaffected by S557A mutation, and S557A-CRY2 protein levels were increased by coexpression of FBXL21 (data not shown). Thus, FBXL21 is less likely to be involved directly in Ser557/Ser553 phosphorylation-dependent degradation of CRY2. Multiple ubiquitination sites in CRY1 and CRY2 (Table 1) are indicative of a complex network of CRY ubiquitination that is important for the circadian clockwork.

Fbxl21 knockout mice showed wheel-running rhythms in DD with a period indistinguishable from that of their wild-type littermates (Figure 2F). On the other hand, the Takahashi laboratory (UT Southwestern, USA) found a point mutation in FBXL21 that causes a shortened period of behavioral rhythms (Yoo et al., 2013, this issue of *Cell*). This short-period phenotype is consistent with our observation on the cellular clock, in which silencing of *Fbxl21* in NIH 3T3 cells significantly shortened the period (Figure 2J). We speculate that *Fbxl21* slows down the oscillation speed and that the difference in phenotypes of *Fbxl21* ablation between behavioral and cellular rhythms (Figures 2F and 2J) may be explained by consolidation of the circadian oscillation in the SCN (Liu et al., 2007). It is noteworthy that *Fbxl21* null mice showed a decrease in wheel-running activities near the subjective dawn (Figure 2G). Thus, *Fbxl21* deficiency appears to also affect the SCN clock function regulating the temporal organization of the behaviors. The profound and complex perturbations in the circadian expression profiles of the clock genes (Figure 3C) might be responsible for this abnormality, though the underlying mechanism has yet to be elucidated.

Fbxl21 knockout in *Fbxl3* null background significantly shortened the long circadian period of the behavioral rhythm of *Fbxl3* null mice (Figure 2). This result can be explained by the antagonizing effects of FBXL21 and FBXL3 on CRY stabilities. Importantly, despite the apparent alleviation of the abnormalities of *Fbxl3* knockout mice in terms of the circadian period and the activity onsets, *Fbxl3*/*Fbxl21* double-knockout mice exhibited unstable circadian behaviors as revealed by the occurrence of arrhythmic mice in DD (three out of ten mice; Figure 2D and Table S1) and by the progressive decline in the periodogram amplitude (Qp) during days 9–28 in DD (Figure 2H). Qp is a measure of robustness of circadian rhythms (Sokolove and Bushell, 1978), and the values were unaltered in *Fbxl3* and *Fbxl21* single-knockout mice in DD (Figure 2H). We conclude that FBXL21 and FBXL3 cooperatively play an essential role for the maintenance of the robust clock oscillation by providing a mechanism counterbalancing CRY1 and CRY2 protein levels.

Here we propose a model in which CRY proteins are regulated by FBXL21 and FBXL3 so as to maintain normal circadian oscillation (Figure 6I). FBXL21-mediated ubiquitination of CRY1 and CRY2 provides an ~12 hr time window for accumulation of CRY proteins in the cytosol when the E-box-dependent transcription is kept active. This idea is supported by the subcellular distribution of FBXL21 (Figure 6E) and by the marked reduction of CRY levels in *Fbxl21*-deficient cells (Figures 3B and 6H). *Fbxl21* transcripts show marked circadian variations in the mouse SCN (Dardente et al., 2008), and *Fbxl21* mRNA levels are high during the mid- to late-subjective day when *Cry1* and *Cry2* mRNA levels increase. It is most likely that FBXL21 plays an important role for temporally organizing the accumulation of translated CRYs in the cytosol. On the other hand, FBXL3 ubiquitinates CRYs predominantly in the nucleus to terminate suppression of the E-box-dependent transcription (Godinho et al., 2007). Collectively, a spatiotemporally fine-tuned balance between stabilization and degradation mediated by FBXL21 and FBXL3, respectively, is essential for coordinating the ~24 hr variation of protein abundance of CRY1 and CRY2, the key players in the transcription-based autoregulatory feedback in the circadian clock.

Ubiquitination-mediated degradation of clock proteins, especially that of the transcriptional repressors, has been highlighted as a key regulatory process in the clockwork of many organisms (Gallego and Virshup, 2007; Baker et al., 2012; Ito et al., 2012). In the present study, we demonstrate that coordination of a destabilizer, FBXL3, with a stabilizer, FBXL21, each acting antagonistically on CRY repressors, is critical for generating the CRY expression dynamics and behavior rhythms. CRY protein levels are critical determinants of the timing of CLOCK-BMAL1-dependent transcriptional activation. Thus, the balance between CRY stabilization and degradation mediated by a combination of FBXL21 and FBXL3 is essential to drive the 24 hr cycle of the circadian clock. Our results underscore an emerging concept that switching between protein degradation and stabilization

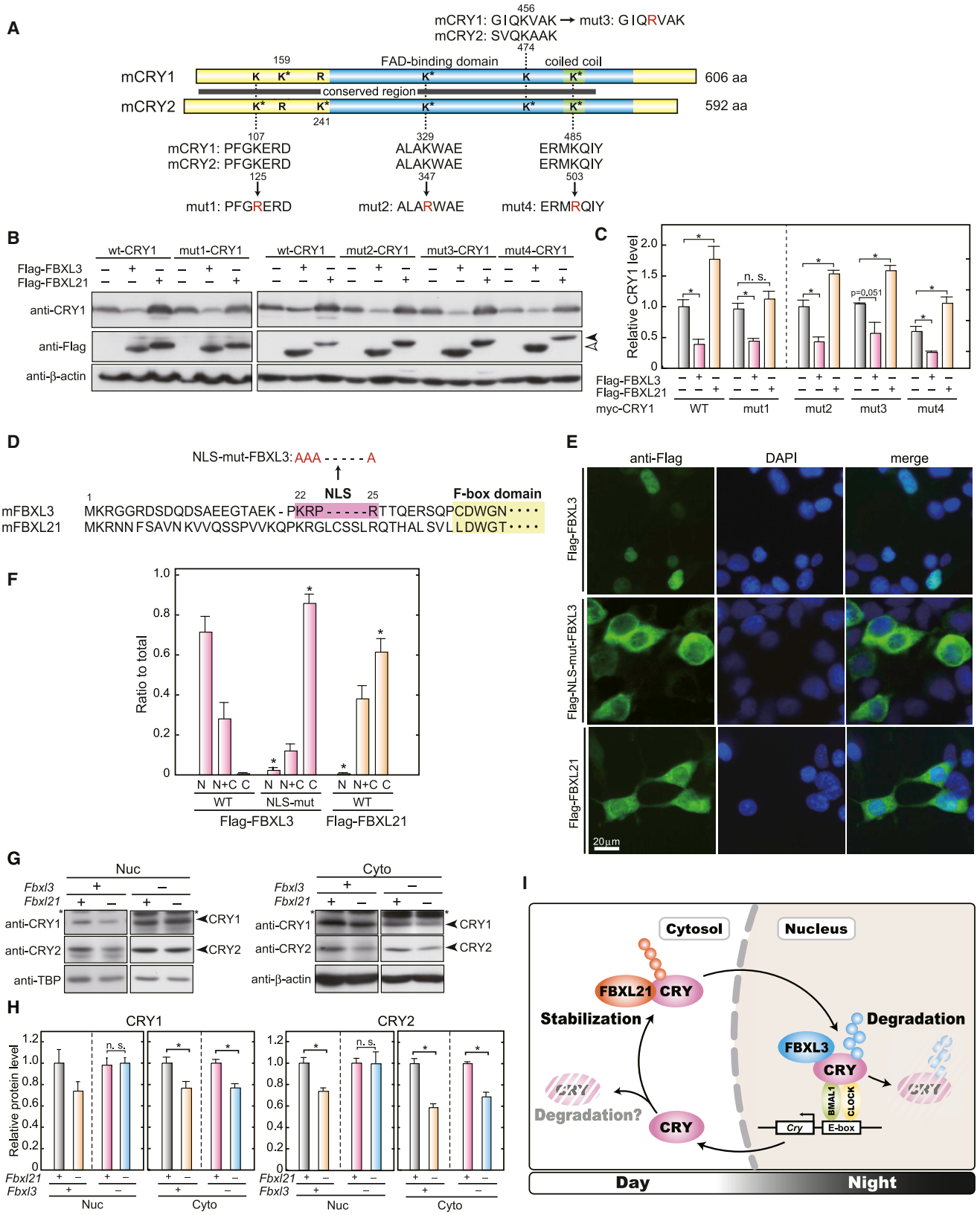

(legend on next page)

directed by posttranslational modifications (Brooks and Gu, 2003; Perkins, 2006) underlies the regulatory processes of many biological events.

EXPERIMENTAL PROCEDURES

Animals

All the mouse experiments were approved by the animal ethics committee of The University of Tokyo and Kyushu University. Mice were housed in cages with free access to commercial chow (CLEA Japan) and tap water. See Extended Experimental Procedures for details on the generation of *Fbxl3*$^{-/-}$ and *Fbxl21*$^{-/-}$ mice.

Wheel-Running Activity

Five- to ten-week-old mice were housed individually in cages equipped with running wheels. The animals were maintained in a light-tight chamber at a constant temperature (23°C ± 1°C) and humidity (65% ± 10%). Mice were entrained to the LD cycle for at least 5 weeks and released into DD for 21 days or longer. Wheel revolutions were recorded in 5 min bins and analyzed with ClockLab analysis software (Actimetrics). The circadian period and periodogram amplitude of the activity rhythms in DD were determined using chi-square periodogram procedure with ClockLab.

Cell Culture and Plasmids for Transfection

MEFs were prepared from E12.5 embryos. After the head, paws, and internal organs were removed, embryos were chopped and incubated in 0.25% trypsin in PBS for 24 hr at 4°C. After incubation for 30 min at 37°C in 0.25% trypsin in PBS, cells were dissociated by pipetting. MEFs, NIH 3T3 (Riken Cell Bank), and HEK293T17 cells were cultured and passaged under 5% CO_2 in DMEM (Nissui) containing 1.8 mg/ml $NaHCO_3$, 4.5 mg/ml glucose, 100 U/ml penicillin, 100 μg/ml streptomycin, and 10% fetal bovine serum (Equitech Bio). NIH 3T3 and HEK293T17 cells were transiently transfected using Lipofectamine Plus reagent (Invitrogen) and Lipofectamine 2000 reagent (Invitrogen), respectively, according to the manufacturer's protocols. Plasmids used for transfection are described in the Extended Experimental Procedures.

Immunoblotting

Proteins separated by SDS-PAGE were transferred to polyvinylidene difluoride membrane (Millipore). The blots were blocked in a blocking solution (1% [w/v] skim milk in TBS [50 mM Tris-HCl, 140 mM NaCl, 1mM $MgCl_2$ (pH 7.4)]) for 1 hr at 37°C and then incubated overnight at 4°C with a primary antibody in the blocking solution. The signals were visualized by an enhanced chemiluminescence detection system (PerkinElmer Life Science). The blot membrane was subjected to densitometric scanning and the band intensities were quantified using Image Gauge Ver.4.0 software (Fujifilm Science Lab). Antibodies were described in the Extended Experimental Procedures.

Degradation Assay

Cells were transfected with FHM- or myc-CRY1 and Flag-FBXLs expression vectors and cultured for 48 hr. The transfected cells were then treated with 100 μg/ml cycloheximide (Nakalai tesque) for time periods specified in the figures and harvested, followed by immunoblotting. Degradation assay in cultured MEFs was performed in essentially the same way except that DNA was not transfected.

SUPPLEMENTAL INFORMATION

Supplemental Information includes three figures, one table, and Extended Experimental Procedures and can be found with this article online at http://dx.doi.org/10.1016/j.cell.2013.01.054.

ACKNOWLEDGMENTS

We thank Kentaro Hirose and Drs. Daisuke Kojima and Masaki Torii for their help with data analysis. We are grateful to Drs. Joseph S. Takahashi and Seung-Hee Yoo for communicating their unpublished results on *Fbxl21* and to Drs. Steve A. Kay and Tsuyoshi Hirota for providing us with CRY1-Luc expression vectors. We also thank Jun Nakano and Drs. Hikari Yoshitane and Kimiko Shimizu for critical comments on the manuscript. This work was supported in part by Grants-in-Aid for Scientific research and by the Global COE program (Integrative Life Science Based on the Study of Biosignaling Mechanisms) from MEXT, Japan. A.H. is supported by JSPS Research Fellowships for Young Scientists.

Received: August 14, 2012
Revised: December 3, 2012
Accepted: January 30, 2013
Published: February 28, 2013

REFERENCES

Baker, C.L., Loros, J.J., and Dunlap, J.C. (2012). The circadian clock of Neurospora crassa. FEMS Microbiol. Rev. *36*, 95–110.

Behrends, C., and Harper, J.W. (2011). Constructing and decoding unconventional ubiquitin chains. Nat. Struct. Mol. Biol. *18*, 520–528.

Brooks, C.L., and Gu, W. (2003). Ubiquitination, phosphorylation and acetylation: the molecular basis for p53 regulation. Curr. Opin. Cell Biol. *15*, 164–171.

Figure 6. Identification of Ubiquitination Sites by Mass Spectrometry Analysis

(A) Ubiquitination sites in CRY1 and CRY2 identified by mass spectrometry analysis. Overexpressed FHM-CRY1 or FHM-CRY2 in NIH 3T3 cells was purified by Flag antibody and subjected to mass spectrometry analysis. Ubiquitinated Lys residues (three residues in CRY1 and five in CRY2) are highlighted with asterisks. The gray horizontal bar indicates a region highly conserved between mouse CRY1 and CRY2.

(B) Effect of coexpression of FBXL3 or FBXL21 on mutant CRY1 protein levels. Mut(1-4)-CRY1 and Flag-FBXLs were expressed in HEK293T17 cells. Steady-state levels of CRY1 protein were determined by immunoblotting analysis with CRY1 antibody. The solid and open arrowheads indicate Flag-FBXL21 and Flag-FBXL3, respectively.

(C) Each mut-CRY1 protein levels were quantified and shown with error bars of SEM (n = 3, *p < 0.05 by Tukey's test).

(D) Mouse FBXL3 has an NLS sequence, which is not conserved in FBXL21.

(E) Intracellular distribution of FBXL3, NLS-mut-FBXL3, and FBXL21. Flag-FBXL3, Flag-NLS-mut-FBXL3, or Flag-FBXL21 was expressed in HEK293T17 cells and immunostained with anti-Flag antibody. Cell nuclei were stained with DAPI.

(F) Quantitative analysis of the subcellular distribution of FBXL3, NLS-mut-FBXL3, and FBXL21. The data were obtained from three independent experiments as in (E), and in each experiment at least 100 cells were visually examined and counted. Data are means + SEM. *p < 0.05 by Tukey's test.

(G) CRY1 and CRY2 protein levels in the mouse cerebrum. The mouse cerebrum lysate prepared at ZT18 were fractionated into the nuclear and cytosolic fraction. The same amounts of proteins (50 μg cytosolic proteins or 20 μg nuclear proteins) were loaded.

(H) The band intensities of CRY1 and CRY2 in (G) were quantified and the highest value was set at 1.0. Data are means + SEM (n = 4, *p < 0.05 by Student's t test).

(I) In the cytosol, FBXL21 stabilizes CRY proteins, probably by counterbalancing a degradation mechanism (in gray). This controls appropriate rate of accumulation of translated CRYs in their increasing phase during the daytime. In the nucleus, FBXL3 leads CRYs to proteasomal degradation, which is also competed by FBXL21-mediated stabilization, in the declining phase of CRYs during the nighttime. Dual regulation of CRY protein stabilities by a combination of FBXL21 and FBXL3 plays a critical role for robust oscillation of the circadian clock.

Bunger, M.K., Wilsbacher, L.D., Moran, S.M., Clendenin, C., Radcliffe, L.A., Hogenesch, J.B., Simon, M.C., Takahashi, J.S., and Bradfield, C.A. (2000). Mop3 is an essential component of the master circadian pacemaker in mammals. Cell *103*, 1009–1017.

Busino, L., Bassermann, F., Maiolica, A., Lee, C., Nolan, P.M., Godinho, S.I., Draetta, G.F., and Pagano, M. (2007). SCFFbxl3 controls the oscillation of the circadian clock by directing the degradation of cryptochrome proteins. Science *316*, 900–904.

Cardozo, T., and Pagano, M. (2004). The SCF ubiquitin ligase: insights into a molecular machine. Nat. Rev. Mol. Cell Biol. *5*, 739–751.

Chen, Z.J., and Sun, L.J. (2009). Nonproteolytic functions of ubiquitin in cell signaling. Mol. Cell *33*, 275–286.

Dardente, H., Mendoza, J., Fustin, J.M., Challet, E., and Hazlerigg, D.G. (2008). Implication of the F-Box Protein FBXL21 in circadian pacemaker function in mammals. PLoS ONE *3*, e3530.

Dunlap, J.C. (1999). Molecular bases for circadian clocks. Cell *96*, 271–290.

Frescas, D., and Pagano, M. (2008). Deregulated proteolysis by the F-box proteins SKP2 and beta-TrCP: tipping the scales of cancer. Nat. Rev. Cancer *8*, 438–449.

Gallego, M., and Virshup, D.M. (2007). Post-translational modifications regulate the ticking of the circadian clock. Nat. Rev. Mol. Cell Biol. *8*, 139–148.

Gekakis, N., Staknis, D., Nguyen, H.B., Davis, F.C., Wilsbacher, L.D., King, D.P., Takahashi, J.S., and Weitz, C.J. (1998). Role of the CLOCK protein in the mammalian circadian mechanism. Science *280*, 1564–1569.

Godinho, S.I., Maywood, E.S., Shaw, L., Tucci, V., Barnard, A.R., Busino, L., Pagano, M., Kendall, R., Quwailid, M.M., Romero, M.R., et al. (2007). The after-hours mutant reveals a role for Fbxl3 in determining mammalian circadian period. Science *316*, 897–900.

Harada, Y., Sakai, M., Kurabayashi, N., Hirota, T., and Fukada, Y. (2005). Ser-557-phosphorylated mCRY2 is degraded upon synergistic phosphorylation by glycogen synthase kinase-3 beta. J. Biol. Chem. *280*, 31714–31721.

Hastings, M.H., Reddy, A.B., and Maywood, E.S. (2003). A clockwork web: circadian timing in brain and periphery, in health and disease. Nat. Rev. Neurosci. *4*, 649–661.

Ito, S., Song, Y.H., and Imaizumi, T. (2012). LOV domain-containing F-box proteins: light-dependent protein degradation modules in Arabidopsis. Mol Plant *5*, 573–582.

Jin, J., Cardozo, T., Lovering, R.C., Elledge, S.J., Pagano, M., and Harper, J.W. (2004). Systematic analysis and nomenclature of mammalian F-box proteins. Genes Dev. *18*, 2573–2580.

Kim, W., Bennett, E.J., Huttlin, E.L., Guo, A., Li, J., Possemato, A., Sowa, M.E., Rad, R., Rush, J., Comb, M.J., et al. (2011). Systematic and quantitative assessment of the ubiquitin-modified proteome. Mol. Cell *44*, 325–340.

Kon, N., Hirota, T., Kawamoto, T., Kato, Y., Tsubota, T., and Fukada, Y. (2008). Activation of TGF-beta/activin signalling resets the circadian clock through rapid induction of Dec1 transcripts. Nat. Cell Biol. *10*, 1463–1469.

Kume, K., Zylka, M.J., Sriram, S., Shearman, L.P., Weaver, D.R., Jin, X., Maywood, E.S., Hastings, M.H., and Reppert, S.M. (1999). mCRY1 and mCRY2 are essential components of the negative limb of the circadian clock feedback loop. Cell *98*, 193–205.

Kurabayashi, N., Hirota, T., Harada, Y., Sakai, M., and Fukada, Y. (2006). Phosphorylation of mCRY2 at Ser557 in the hypothalamic suprachiasmatic nucleus of the mouse. Chronobiol. Int. *23*, 129–134.

Kurabayashi, N., Hirota, T., Sakai, M., Sanada, K., and Fukada, Y. (2010). DYRK1A and glycogen synthase kinase 3beta, a dual-kinase mechanism directing proteasomal degradation of CRY2 for circadian timekeeping. Mol. Cell. Biol. *30*, 1757–1768.

Lamia, K.A., Sachdeva, U.M., DiTacchio, L., Williams, E.C., Alvarez, J.G., Egan, D.F., Vasquez, D.S., Juguilon, H., Panda, S., Shaw, R.J., et al. (2009). AMPK regulates the circadian clock by cryptochrome phosphorylation and degradation. Science *326*, 437–440.

Liu, A.C., Welsh, D.K., Ko, C.H., Tran, H.G., Zhang, E.E., Priest, A.A., Buhr, E.D., Singer, O., Meeker, K., Verma, I.M., et al. (2007). Intercellular coupling confers robustness against mutations in the SCN circadian clock network. Cell *129*, 605–616.

Nolan, P.M., and Parsons, M.J. (2009). Clocks go forward: progress in the molecular genetic analysis of rhythmic behaviour. Mamm. Genome *20*, 67–70.

Pan, Z.Q., Kentsis, A., Dias, D.C., Yamoah, K., and Wu, K. (2004). Nedd8 on cullin: building an expressway to protein destruction. Oncogene *23*, 1985–1997.

Perkins, N.D. (2006). Post-translational modifications regulating the activity and function of the nuclear factor kappa B pathway. Oncogene *25*, 6717–6730.

Popov, N., Schülein, C., Jaenicke, L.A., and Eilers, M. (2010). Ubiquitylation of the amino terminus of Myc by SCF(β-TrCP) antagonizes SCF(Fbw7)-mediated turnover. Nat. Cell Biol. *12*, 973–981.

Reischl, S., and Kramer, A. (2011). Kinases and phosphatases in the mammalian circadian clock. FEBS Lett. *585*, 1393–1399.

Schibler, U., and Sassone-Corsi, P. (2002). A web of circadian pacemakers. Cell *111*, 919–922.

Shearman, L.P., Sriram, S., Weaver, D.R., Maywood, E.S., Chaves, I., Zheng, B., Kume, K., Lee, C.C., van der Horst, G.T., Hastings, M.H., and Reppert, S.M. (2000). Interacting molecular loops in the mammalian circadian clock. Science *288*, 1013–1019.

Siepka, S.M., Yoo, S.H., Park, J., Song, W., Kumar, V., Hu, Y., Lee, C., and Takahashi, J.S. (2007). Circadian mutant Overtime reveals F-box protein FBXL3 regulation of cryptochrome and period gene expression. Cell *129*, 1011–1023.

Sokolove, P.G., and Bushell, W.N. (1978). The chi square periodogram: its utility for analysis of circadian rhythms. J. Theor. Biol. *72*, 131–160.

Takahashi, J.S. (1995). Molecular neurobiology and genetics of circadian rhythms in mammals. Annu. Rev. Neurosci. *18*, 531–553.

Toh, K.L., Jones, C.R., He, Y., Eide, E.J., Hinz, W.A., Virshup, D.M., Ptácek, L.J., and Fu, Y.H. (2001). An hPer2 phosphorylation site mutation in familial advanced sleep phase syndrome. Science *291*, 1040–1043.

Yoo, S.-H., Mohawk, J.A., Siepka, S.M., Shan, Y., Huh, S.K., Hong, H.-K., Kornblum, I., Kumar, V., Koike, N., Xu, M., et al. (2013). Competing E3 ubiquitin ligases govern circadian periodicity by degradation of CRY in nucleus and cytoplasm. Cell *152*, this issue, 1091–1105.

van der Horst, G.T., Muijtjens, M., Kobayashi, K., Takano, R., Kanno, S., Takao, M., de Wit, J., Verkerk, A., Eker, A.P., van Leenen, D., et al. (1999). Mammalian Cry1 and Cry2 are essential for maintenance of circadian rhythms. Nature *398*, 627–630.